ARMY RESEARCH LABORATORY

Air Blast Calculations

by Joel B. Stewart

ARL-TN-549 July 2013

NOTICES

Disclaimers

The findings in this report are not to be construed as an official Department of the Army position unless so designated by other authorized documents.

Citation of manufacturer's or trade names does not constitute an official endorsement or approval of the use thereof.

Destroy this report when it is no longer needed. Do not return it to the originator.

Army Research Laboratory

Aberdeen Proving Ground, MD 21005-5066

ARL-TN-549 **July 2013**

Air Blast Calculations

Joel B. Stewart

Weapons and Materials Research Directorate, ARL

REPORT DOCUMENTATION PAGE	Form Approved OMB No. 0704-0188

1. REPORT DATE *(DD-MM-YYYY)*	2. REPORT TYPE	3. DATES COVERED (From - To)
July 2013	Final	March 2012–April 2012

4. TITLE AND SUBTITLE
Air Blast Calculations

5a. CONTRACT NUMBER

5b. GRANT NUMBER

5c. PROGRAM ELEMENT NUMBER

6. AUTHOR(S)
Joel B. Stewart

5d. PROJECT NUMBER
AH80

5e. TASK NUMBER

5f. WORK UNIT NUMBER

7. PERFORMING ORGANIZATION NAME(S) AND ADDRESS(ES)
U.S. Army Research Laboratory
ATTN: RDRL-WMP-G
Aberdeen Proving Ground, MD 21005-5069

8. PERFORMING ORGANIZATION REPORT NUMBER
ARL-TN-549

9. SPONSORING/MONITORING AGENCY NAME(S) AND ADDRESS(ES)

10. SPONSOR/MONITOR'S ACRONYM(S)

11. SPONSOR/MONITOR'S REPORT NUMBER(S)

12. DISTRIBUTION/AVAILABILITY STATEMENT
Approved for public release; distribution is unlimited.

13. SUPPLEMENTARY NOTES
Author email: <joel.b.stewart2.civ@mail.mil>

14. ABSTRACT
When an explosive detonates, the rapid expansion of reaction gases generates a shock wave that propagates into the surrounding medium. The pressure history at a given spatial location generally consists of an early positive (compressive) phase followed by a negative phase. This technical note documents a series of air blast calculations, using the Sandia hydrocode CTH, aimed at determining the pressure time histories at various gauge locations away from a spherical explosive charge suspended in air. A comparison of the results obtained using CTH are made to ones generated using the Friedlander approximation.

15. SUBJECT TERMS
air blast, CTH, Friedlander

16. SECURITY CLASSIFICATION OF:			17. LIMITATION OF ABSTRACT	18. NUMBER OF PAGES	19a. NAME OF RESPONSIBLE PERSON
a. REPORT	b. ABSTRACT	c. THIS PAGE			Joel B. Stewart
Unclassified	Unclassified	Unclassified	UU	24	19b. TELEPHONE NUMBER (*Include area code*) 410-278-3129

Contents

List of Figures

List of Tables

1. Introduction

When an explosive detonates, the rapid expansion of reaction gases generates a shock wave that propagates into the surrounding medium (assumed in this note to be air). The pressure history at a given spatial location generally consists of an early positive (compressive) phase followed by a negative phase. This negative phase results from the inertial effects of air. The air takes time to accelerate when the shock wave arrives, and once the shock wave passes, the air shifts back toward the comparatively still air behind it, resulting in the negative-pressure phase relative to ambient conditions (*1*).

This technical note documents a series of air blast calculations aimed at determining the pressure histories at various gauge locations away from a spherical explosive charge suspended in air. Four different explosives are considered: trinitrotoluene (TNT), composition C-4 (C4), a polymer-bonded explosive (PBXN-109), and nitromethane (NM). Each charge diameter (CD) is assumed to be 17.46 cm (equivalent to a 10-lb charge for the TNT case). All calculations are completed using the Sandia hydrocode CTH (*2*), with model parameters provided in the code's material library. A Jones-Wilkins-Lee (JWL) equation of state is used for each explosive considered, and a Sesame tabular equation of state is used to model the air behavior. A comparison of the results obtained using CTH is made to ones generated using the Friedlander approximation (*3*).

Some of the explosives investigated herein exhibit nonideal behavior (e.g., PBXN-109). The JWL model used to predict the expansion of the reactant products does not necessarily capture this nonideal behavior (e.g., the JWL model cannot generally account for the energy added to the shock due to late-time burning of the aluminum particles in PBXN-109). Since all of the features of reaction for these materials are not accounted for in the JWL model, the reader should be cautious about directly using the results—especially in regions where the inherent assumptions break down.

Because one of the main objectives of this note is to compare the CTH calculations to the Friedlander approximation, the explosive behavior is described using programmed burn with a JWL model governing the product expansion. This reaction model is chosen both because it is the most commonly used model in the hydrocodes to describe explosive behavior and because it is one of the simpler models available. The rationale behind using programmed burn along with the JWL model to describe the explosive behavior is that if the Friedlander approximation cannot

match the results from even one of the simpler reaction models, there is little hope that it will be able to handle more complex situations (such as late-time burning of metallic particles). Ultimately, when using the Friedlander equation (or any other model), the analyst should be aware of the underlying assumptions inherent in the model equations.

2. Results

All calculations presented in this report assumed a spherical explosive charge, with a CD equal to 17.46 cm, suspended in air and detonated at the center. Because of the spherical symmetry of the problem, all the CTH analyses were 1-D spherical calculations. A JWL equation of state was assumed for each of the four explosives investigated (TNT, C4, PBXN-109, and NM) and the CTH material library parameters were used for each. Air was modeled using the Sesame tabular equation of state available in the CTH material library. A converged solution was obtained by using one computational cell per millimeter. Pressure time histories were taken at 5, 10, 20, and 60 CDs (i.e., at 87.3, 174.6, 349.2, and 1047.6 cm, measured from the center of the spherical charge).

Figures 1–4 depict at 5, 10, 20, and 60 CDs, respectively, the initial shock wave for each of the four explosives investigated. The profiles of the four explosives are seen to be qualitatively similar, with PBXN-109 and C4 generating the largest overpressures at each gauge location, followed by TNT and NM with somewhat lower pressures (see table 1). The overpressure drops off substantially by 20 CDs (note that the ambient pressure is 100 kPa such that overpressure is measured relative to this pressure). The extent of the initial signal's negative phase is tabulated in table 2 for the four different explosives investigated at the four different gauge locations.

Table 1. Peak overpressure (in kilopascal).

Gauge Distance	TNT	C4	PBXN-109	NM
5 CD	3178	3972	4031	2694
10 CD	762	924	985	600
20 CD	140	161	170	113
60 CD	20	22	22	17

The curves in figure 1, which were captured from gauges located at 5 CDs from the explosive,

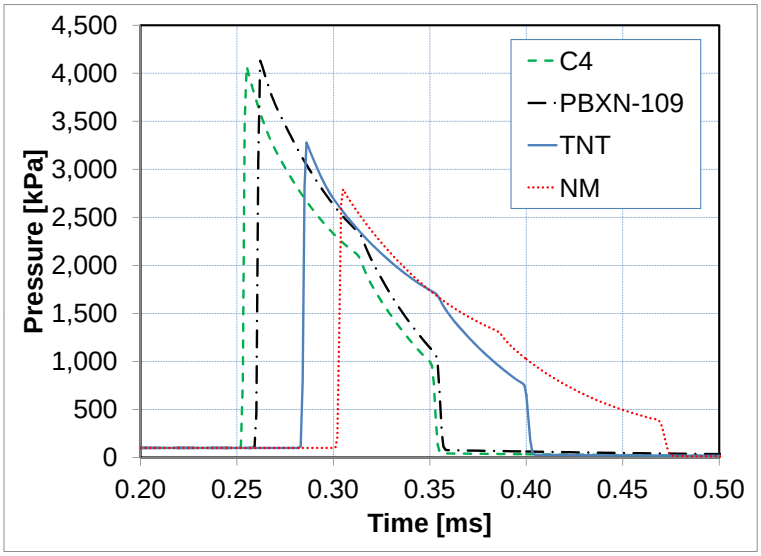

Figure 1. Pressure gauge time histories for various explosive charges at 5 CDs.

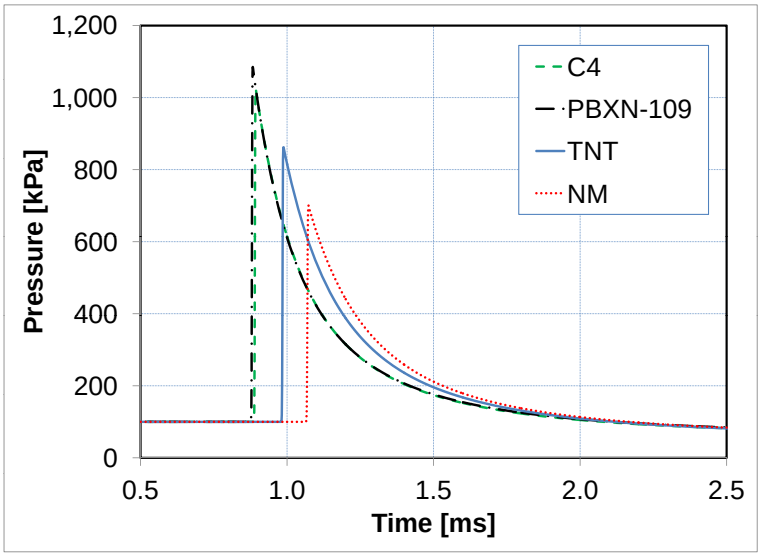

Figure 2. Pressure gauge time histories for various explosive charges at 10 CDs.

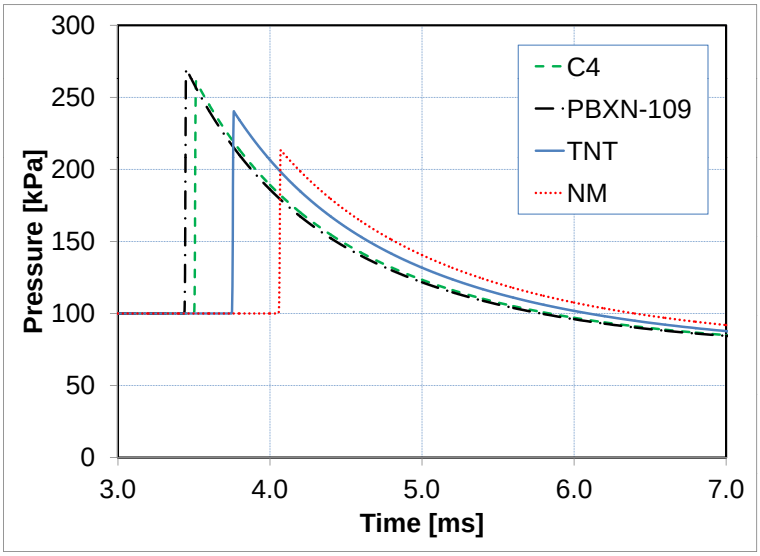

Figure 3. Pressure gauge time histories for various explosive charges at 20 CDs.

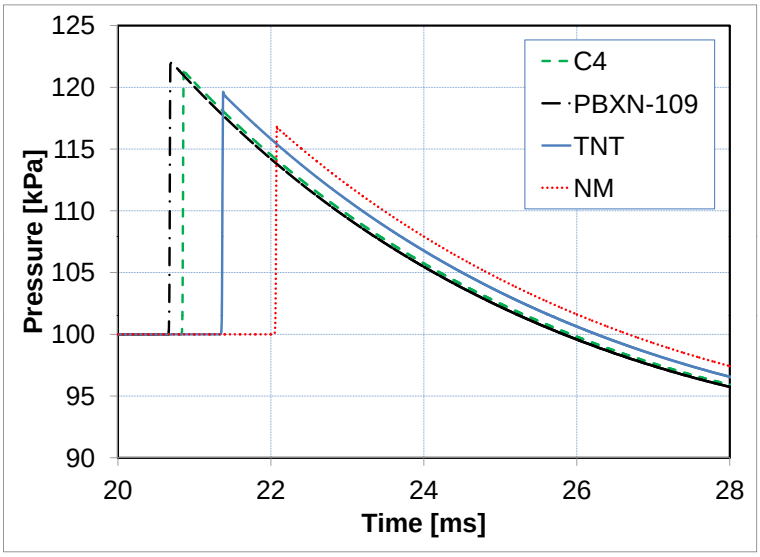

Figure 4. Pressure gauge time histories for various explosive charges at 60 CDs.

Table 2. Maximum difference from ambient pressure (in kilopascal) in the negative-pressure phase.

Gauge Distance	TNT	C4	PBXN-109	NM
5 CD	-99	-99	-98	-98
10 CD	-35	-30	-28	-33
20 CD	-21	-21	-21	-19
60 CD	-6	-6	-6	-6

display some different behavior when compared to the time histories captured further away from the charges. To understand the pressure time histories at this gauge nearest to the explosive, the pressure time histories of all gauges in the C4 case during the first 30 ms are shown in figure 5 as a log-log plot. The time histories at 5 CDs are characterized by 1) an early peak (around 0.25 ms in figure 5), which is due to the initial shock from the detonation; 2) an inflection point (around 0.31 ms), which is due to the interface between the highly compressed shell of air behind the initial shock and in front of the explosive products; and 3) a steep pressure drop (around 0.35 ms), which is due to a developing, inward-moving shock being dragged along with the detonation products (i.e., the products containing this developing shock are initially moving faster away from the center than the shock is moving toward it). The secondary shock eventually gets through the fast-moving detonation products (seen as a shock around 1.3 ms), reflects off the center of the spherically detonated charge, and is seen at later times and gauges further out as a weaker shock behind the primary one (e.g., this reflected shock is seen around 3.3 ms at the 5 CD gauge in figure 5). For further discussion of this phenomena near the charge, the reader is referred to discussions in (*4*).

A Friedlander waveform is often used to describe the blast overpressure once the blast wave has fully developed (i.e., at some distance away from the detonated charge). This waveform assumes that there are no nearby surfaces for the blast wave to reflect off of, which is an appropriate assumption for the calculations performed in this current work. The Friedlander waveform is given as follows:

$$P\left(t\right) = P_s e^{\frac{-t}{t^*}} \left(1 - \frac{t}{t^*}\right), \tag{1}$$

where P_s is the peak overpressure and t^* is the time it takes for the overpressure to reach ambient pressure. Figures 6–13 contain a comparison of the results obtained from the CTH calculations and those obtained using the Friedlander equation (equation [1]). The figures are broken up for clarity, with figures 6–9 containing the plots for C4 and TNT, while figures 10–13 contain the plots for PBXN-109 and NM. Figures 6, 7, 10, and 11 show that the Friedlander waveform

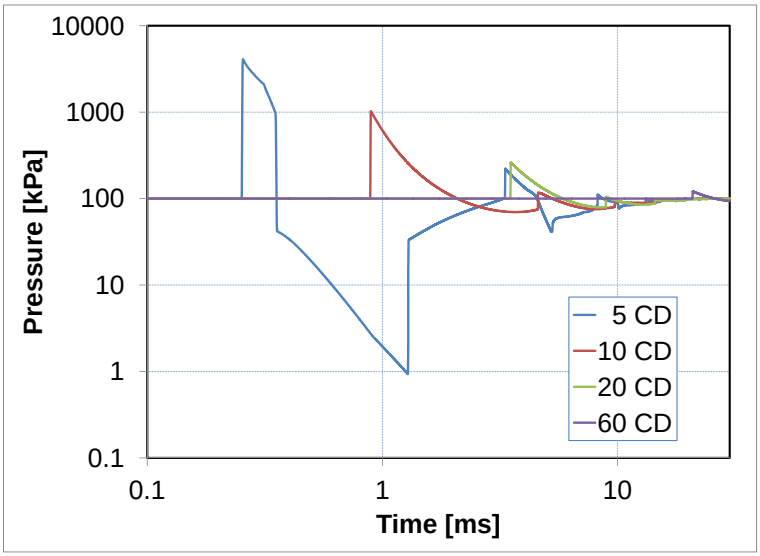

Figure 5. C4 pressure time histories (log-log) at various gauge locations.

provides a poor approximation close to the detonated charge; however, the Friedlander equation gives reasonable results at 20 CDs and greater away from the explosive charge (see figures 8, 9, 12, and 13).

That the Friedlander equation (equation [1]) results in a poor approximation to the pressures seen at 5 CDs (i.e., figures 6 and 10) is not terribly surprising; the Friedlander equation is meant for tracking developed shocks through air, while the gauges at this point are still inside the explosive fireball (where the pressure time histories are dramatically influenced by the propagating interface between the explosive products and air as well as the inward-moving shock generated by the over-expanded gases). The gauges at 10 CDs appear to be outside of the explosive fireball (since no evidence of an air-product interface is detected in any of the pressure time histories at this point); however, the lack of agreement between the Friedlander equation and the CTH results is still understandable since the Friedlander equation is inaccurate for overpressures much above 1 atm, or roughly 100 kPa, and a modified Friedlander equation is often used instead (*3*).

The curves shown in figures 14–17 illustrate the impulse per unit area (i.e., the integral of the pressure time histories) calculated from the pressure data for each explosive at each of the four gauges. The qualitative behavior of the impulses is similar for the four different explosives, with PBXN-109 resulting in the highest impulses and NM yielding the lowest. The impulse obtained

using the Friedlander approximation of equation 1 is also shown for comparison with the CTH results. Once again, the Friedlander approximation gives a reasonable agreement with the CTH results (comparing up to the peak impulse) between 20 and 60 CDs but gives less than ideal agreement closer to the explosive charge.

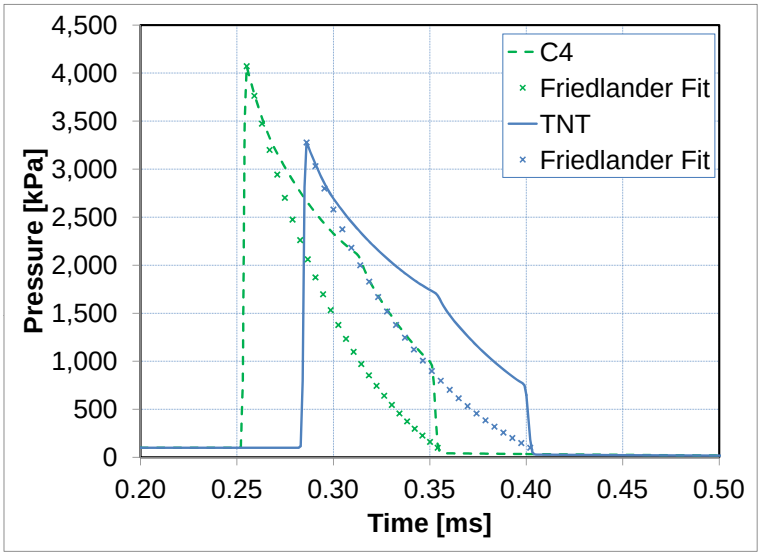

Figure 6. Pressure gauge time histories with the corresponding fit to the Friedlander waveform at 5 CDs for C4 and TNT.

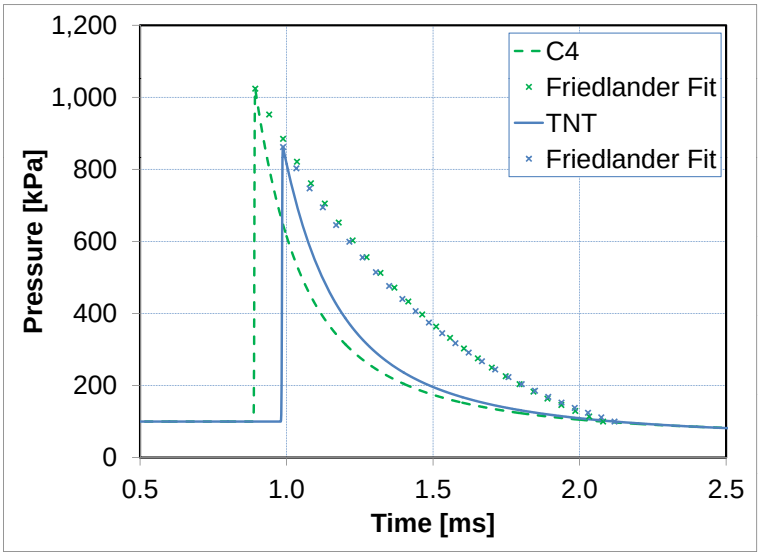

Figure 7. Pressure gauge time histories with the corresponding fit to the Friedlander waveform at 10 CDs for C4 and TNT.

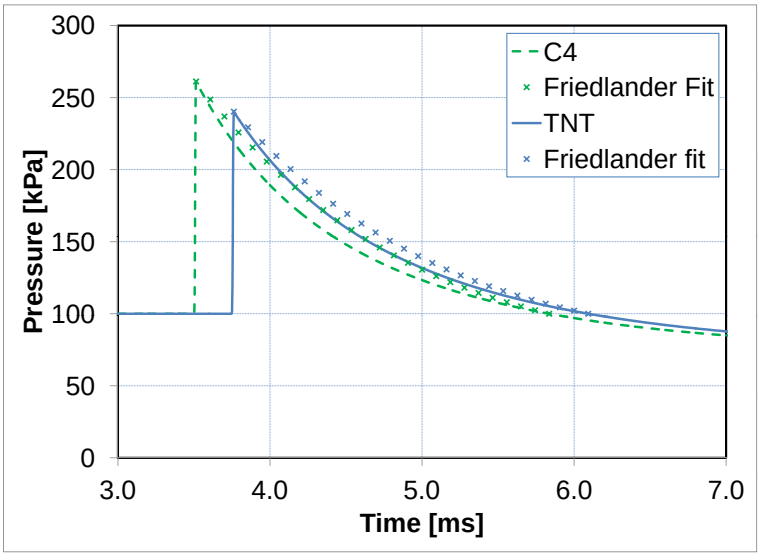

Figure 8. Pressure gauge time histories with the corresponding fit to the Friedlander waveform at 20 CDs for C4 and TNT.

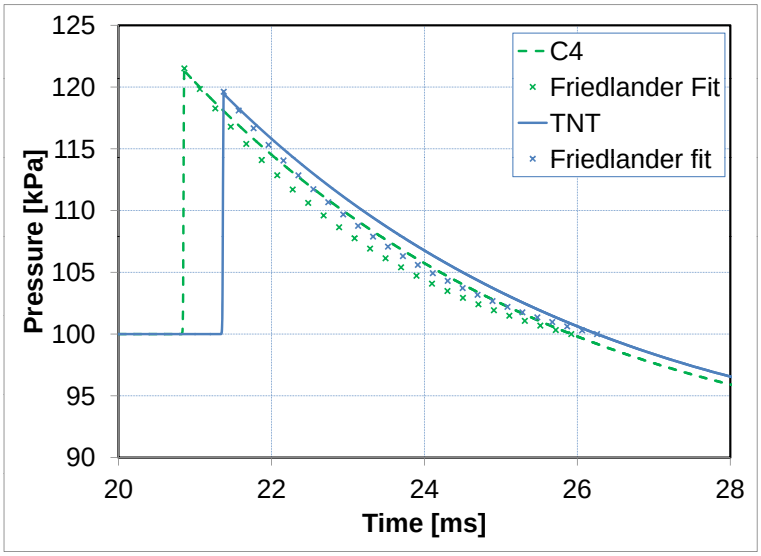

Figure 9. Pressure gauge time histories with the corresponding fit to the Friedlander waveform at 60 CDs for C4 and TNT.

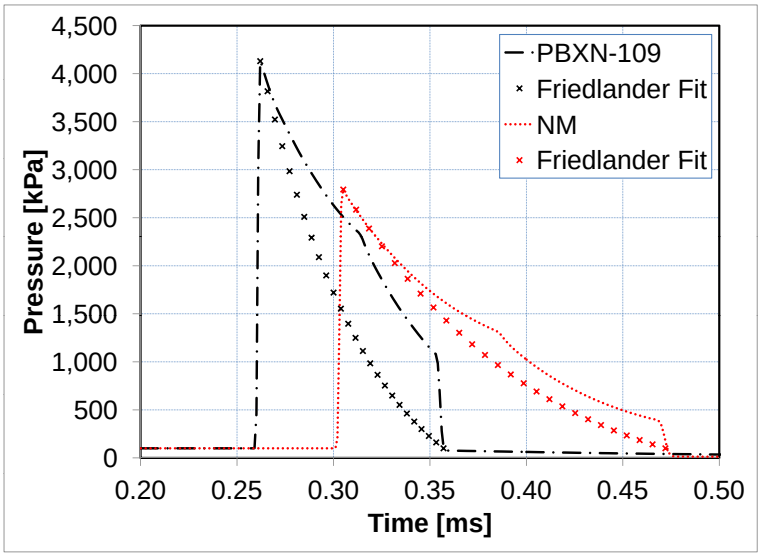

Figure 10. Pressure gauge time histories with the corresponding fit to the Friedlander waveform at 5 CDs, for PBXN-109 and NM.

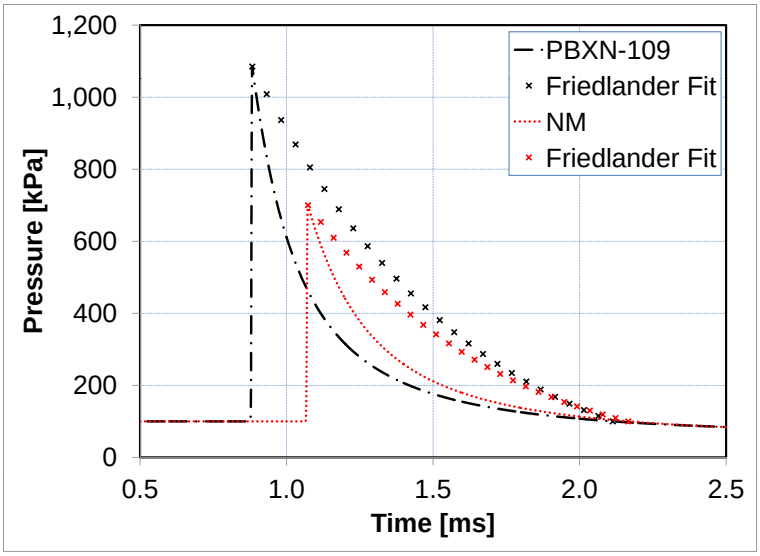

Figure 11. Pressure gauge time histories with the corresponding fit to the Friedlander waveform at 10 CDs for PBXN-109 and NM.

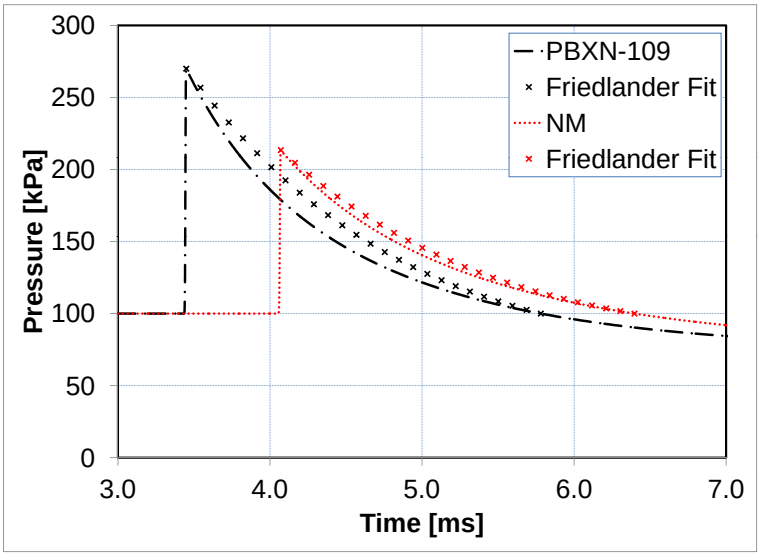

Figure 12. Pressure gauge time histories with the corresponding fit to the Friedlander waveform at 20 CDs for PBXN-109 and NM.

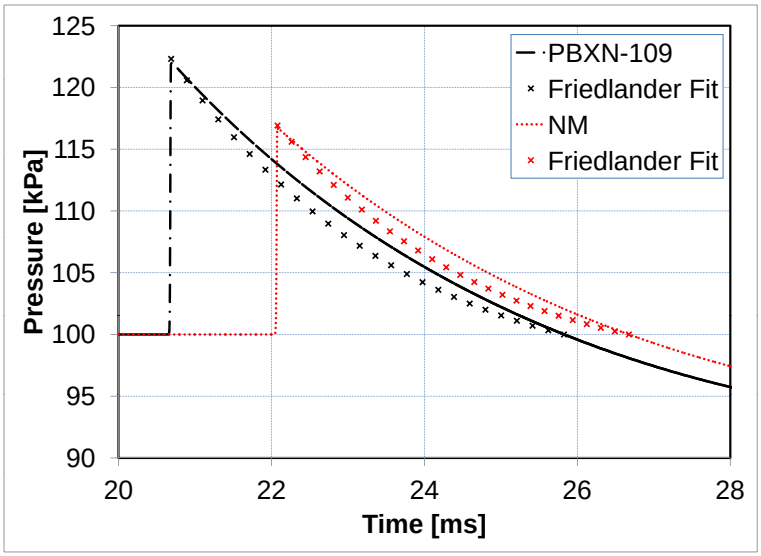

Figure 13. Pressure gauge time histories with the corresponding fit to the Friedlander waveform at 60 CDs for PBXN-109 and NM.

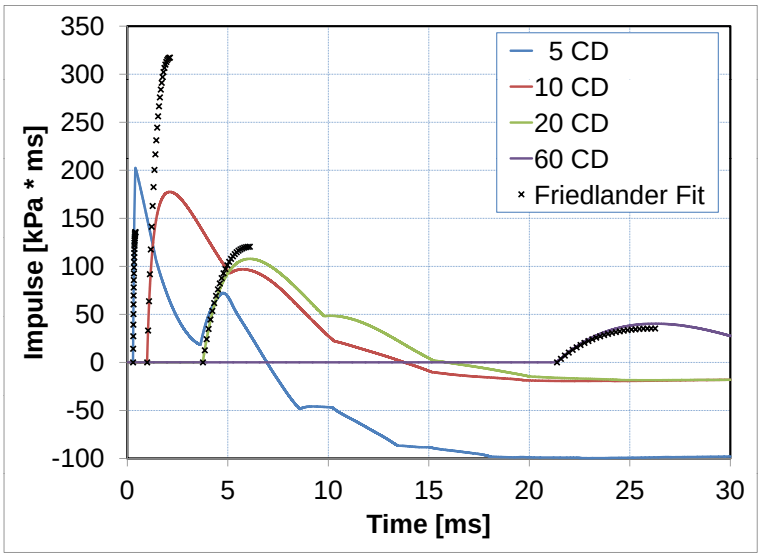

Figure 14. TNT impulse time histories at the four gauge locations along with the Friedlander approximations.

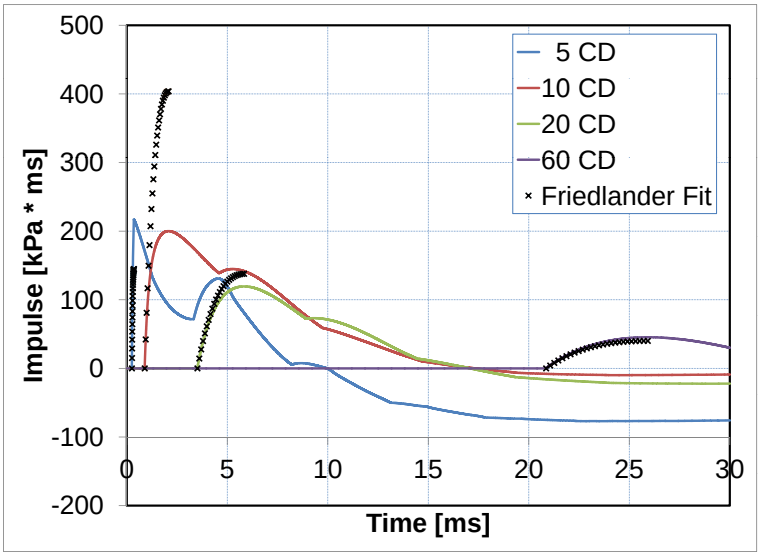

Figure 15. C4 impulse time histories at the four gauge locations along with the Friedlander approximations.

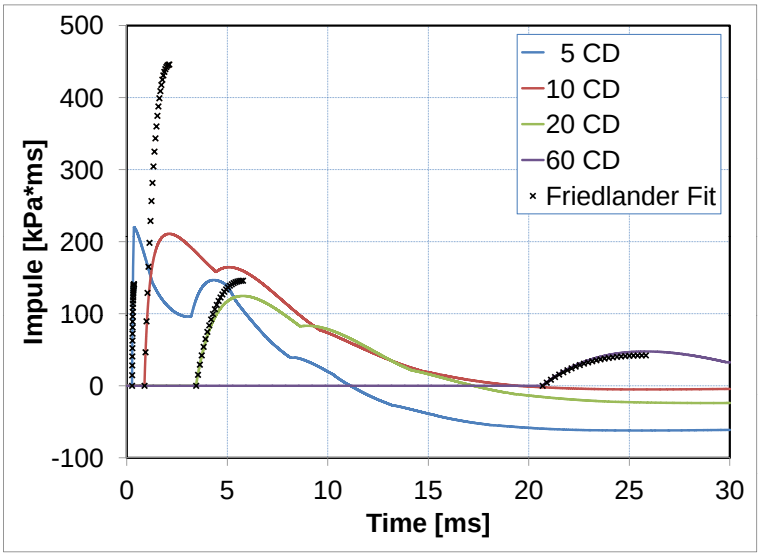

Figure 16. PBXN-109 impulse time histories at the four gauge locations along with the Friedlander approximations.

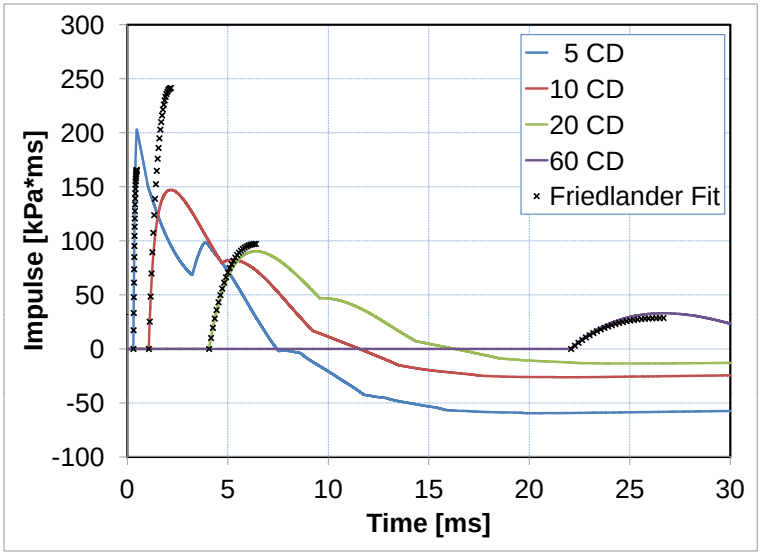

Figure 17. NM impulse time histories at the four gauge locations along with the Friedlander approximations.

3. Summary

In conclusion, four different calculations of spherical explosive charges (TNT, C4, PBXN-109, and NM) were performed using the CTH hydrocode to investigate the pressure time histories at four different gauge locations (5, 10, 20, and 60 CDs). The overpressure was observed to depend both on the explosive used and, especially, on the distance from the explosive charge. Using a Friedlander approximation provided reasonable agreement for pressure decay and integrated impulse at 20 CDs and beyond regardless of the explosive type (ideal or nonideal). In the near-field (5 CDs) and mid-field (10 CDs) regions, the Friedlander approximations were not very accurate; however, the deviation from the CTH results was similar across ideal and nonideal explosive types.

4. References

1. Cooper, P. W. *Explosives Engineering*; Wiley-VCH, Inc.: New York, 1996.

2. Crawford, D. A.; Brundage, A. L.; Harstad, E. N.; Ruggirello, K.; Schmidt, R. G.; Schumacher, S. C.; Simmons, J. S. *CTH User's Manual and Input Instructions, Version 10.2*; Sandia National Laboratories: Albuquerque, NM, January 2012.

3. Dewey, J. M. The Shape of the Blast Wave: Studies of the Friedlander Equation. In *Proceedings of the 21st International Symposium on Military Aspects of Blast and Shock*, 2010.

4. Needham, C. E. *Blast Waves*; Springer-Verlag: Berlin, 2010.

NO. OF COPIES	ORGANIZATION
1 (PDF)	DEFENSE TECHNICAL INFORMATION CTR DTIC OCA
1 (PDF)	DIRECTOR US ARMY RESEARCH LAB RDRL CIO LL
1 (PDF)	DIRECTOR US ARMY RESEARCH LAB IMAL HRA
1 (PDF)	GOVT PRINTG OFC A MALHOTRA
1 (PDF)	US AIR FORCE RESEARCH LABORATORY MUNITIONS DIRECTORATE A OHRT
1 (PDF)	APPLIED RESEARCH ASSOC INC M BROWN
2 (PDF)	DEPARTMENT OF THE NAVY INDIAN HEAD DIVISION, NSWC J CARNEY R LEE
1 (PDF)	DIRECTOR LLNL A KUHL

NO. OF COPIES	ORGANIZATION
	ABERDEEN PROVING GROUND
16 (PDF)	DIR USARL RDRL SLB W P GILLICH C KENNEDY RDRL WMP S SCHOENFELD RDRL WMP A R MUDD RDRL WMP B C HOPPEL RDRL WMP C T BJERKE RDRL WMP D J RUNYEON RDRL WMP E P SWOBODA RDRL WMP F E FIORAVANTE N GNIAZDOWSKI RDRL WMP G R BANTON R EHLERS N ELDREDGE B HOMAN B KRZEWINSKI S KUKUCK

INTENTIONALLY LEFT BLANK.